

*Electronic Supplementary Information (ESI)*

**One-step synthesis and growth mechanism of nitrate intercalated ZnAl LDH conversion coating on zinc**

Aliaksandr Mikhailau<sup>a</sup>, Hanna Malтанава<sup>ab</sup>, Sergei K. Poznyak<sup>b</sup>, Andrei N. Salak<sup>a</sup>, Mikhail Zheludkevich<sup>c</sup>, Kiryl A Yasakau<sup>a\*</sup>, Mário G. S. Ferreira<sup>a</sup>

<sup>a</sup> *Department of Materials and Ceramic Engineering, CICECO - Aveiro institute of materials, University of Aveiro, 3810-193 Aveiro, Portugal.*

<sup>b</sup> *Research Institute for Physical Chemical Problems, Belarusian State University, 220030 Minsk, Belarus.*

<sup>c</sup> *Magnesium Innovations Centre (MagIC), Helmholtz-Zentrum Geesthacht, Germany.*

## Experimental

### Materials and reagents

Zinc foil 2 mm thick as rolled purchased from GoodFellow Cambridge Ltd. having 99.95 wt. % of zinc was used as the substrate. Zinc samples cut in 2×2.5 cm rectangles were abraded with SiC papers down to P360 grit using 2-propanol, cleaned by sonication in 2-propanol, dried in a compressed air flow and stored in a desiccator.

Aluminum nitrate nonahydrate ( $\text{Al}(\text{NO}_3)_3 \cdot 9\text{H}_2\text{O}$ ,  $\geq 98.5\%$ , Sigma Aldrich), sodium nitrate ( $\text{NaNO}_3$ ,  $\geq 99.5\%$ , Sigma Aldrich), ethylenediaminetetraacetic acid disodium salt dihydrate (EDTA,  $\text{C}_{10}\text{H}_{14}\text{N}_2\text{O}_8 \cdot 2\text{H}_2\text{O}$ ,  $\geq 97\%$ , Fluka Analytical), eriochrome black T ( $\text{C}_{20}\text{H}_{12}\text{N}_3\text{NaO}_7\text{S}$ ,  $> 95$ , Alfa Aesar), zinc sulfate heptahydrate ( $\text{ZnSO}_4 \cdot 7\text{H}_2\text{O}$ ,  $\geq 99.5\%$ , Fluka), ethanol ( $\text{C}_2\text{H}_5\text{OH}$ ,  $\geq 99.9\%$ , VWR), dithizone ( $\text{C}_{13}\text{H}_{12}\text{N}_4\text{S}$ , 98%, Alfa Aesar), sodium acetate ( $\text{C}_2\text{H}_4\text{ONa}$ , 99%, Sigma Aldrich) potassium permanganate ( $\text{KMnO}_4$ ,  $\geq 99.5\%$ , Panreac), and sulfuric acid ( $\text{H}_2\text{SO}_4$ ,  $\geq 95\%$ , Honeywell Fluka) were used without additional purification. Deionized water (conductivity  $> 18 \text{ M}\Omega$ ) was used for preparation of solutions and experimental procedures.

### LDH growth method

The LDH synthesis procedure involved several steps. A cleaned zinc substrate was immersed in the solution containing 1 mM aluminum nitrate and 0.1 M sodium nitrate. The solution was heated in a closed vessel at 90°C temperature maintained by a thermostat. The synthesis has been stopped at different time intervals i.e. 1h, 3h, 6h, 9h, 12h and 20h by taking the metallic sample out of the vessel followed by rinsing with deionized water and drying in the flow of compressed air. The samples have been stored in a desiccator, and the solution has been sealed and left for the subsequent analyses described below.

### Examination methods

Phase content and crystal structure of the samples were studied by X-ray diffraction (XRD). Diffraction data was collected at room temperature using a Philips X'Pert MPD diffractometer (Bragg–Brentano geometry, CuK $\alpha$  radiation, tube power 40 kV, 50 mA; X'celerator detector, the exposition corresponded to 11 s per step of  $0.02^\circ \theta$  over the angular range of  $4^\circ < 2\theta < 65^\circ$ ).

Particle morphology and composition were characterized by Scanning Electron Microscopy with Energy Dispersive Spectroscopy (SEM-EDS) using Hitachi S-4100 microscope with electron beam energy of 15-25 kV.

Atomic Force Microscopy (AFM) analysis was performed with a Digital instruments Nanoscope III instrument equipped with extended electronic module in contact mode using silicon nitride probes with reflective gold back coating, spring constant 0.12 N/m, purchased from Veeco.

The pH of the solutions was measured using a pH meter (Mettler Toledo S20, pH electrode InLab® Expert Pro). The pH measurement was done after cooling the solution to the room temperature. Prior to each set of measurements pH meter was calibrated using commercial buffer solutions pH 4.01, 7.00 and 10.00.

Elemental analysis of Zn/Al ratio was performed by analyzing the LDH powder which was detached from the sample by gentle sonication. The titration method described below was used. The LDH powder was dissolved by nitric acid and the pH was adjusted to slightly acidic.

### **Titration methods**

The concentration of zinc and aluminum in the solutions after synthesis was determined by the reverse complexometric titration method as follows. Before performing a titration all the samples were decanted for better accuracy, as some had minor precipitates of LDH from the substrate.

To determine *zinc* concentration 1.00 ml ( $V_{EDTA}$ ) of ~0.02 M EDTA ( $C_{EDTA}$ ) solution<sup>1</sup> was added to 10.0 ml aliquot ( $V_{aliquot}$ ) of the solution analyzed, and the mixture was boiled. Afterwards, a few drops of eriochrome black T water solution and ammonia solution were added to the mixture, and under continuous stirring the solution was titrated with 0.50 mM ZnSO<sub>4</sub> ( $C_{ZnSO_4}$ ) solution. During the titration the solution was maintained hot. The point of equivalence was estimated by visual color change from light blue to purple. The concentration of zinc ( $C_{Zn}$ ) was determined by the volume of titrant added ( $V_{T1}$ ) using following equation:

$$C_{Zn} = (V_{EDTA}C_{EDTA} - V_{T1}C_{ZnSO_4})/V_{aliquot}$$

The concentration of *aluminum* was determined as a difference between the total concentration of metals and zinc ( $C_{Zn}$ ), as we assume no metals except from aluminum and zinc

---

<sup>1</sup> The concentration of EDTA is approximate and must be determined by the titration with metal solution.

are present. To determine total concentrations of metals 1.00 ml ( $V_{EDTA}$ ) of ~0.02 M EDTA solution was added to 10.0 ml aliquot ( $V_{aliquot}$ ) of the solution analyzed, and the mixture was boiled. After the aliquot was cooled in a water bath, 20 ml of ethanol, a few drops of 0.1 M sodium acetate and ethanol solution of dithizone were added to the mixture. The solution was titrated with 0.50 mM  $ZnSO_4$  ( $C_{ZnSO_4}$ ) under stirring. The point of equivalence was estimated by visual color change from weak yellow to peach. The concentration of aluminum ( $C_{Al}$ ) was calculated by the following equation:

$$C_{Al} = (V_{EDTA}C_{EDTA} - V_{T2}C_{ZnSO_4})/V_{aliquot} - C_{Zn}$$

The concentration of reducing agents such as  $NO_2^-$  was determined by the reverse permanganometry. In this method a 10.0 ml aliquot of the solution was mixed with 15.0 ml of 0.80-1.00 mM standardized<sup>2</sup>  $KMnO_4$  solution and a few drops of concentrated sulfuric acid and left for 10-15 minutes. Thereafter the solution was mixed with 2.00 ml of 0.02 M oxalic acid and heated until the solution had discolored. The final solution was titrated warm with the same potassium permanganate solution. The point of equivalence is achieved when the added titrant colors the solution and the color does not disappear during 1-2 minutes of heating. The concentration of the reducing agent was calculated by the following equation:

$$C_{NO_2^-} = [5(V_{KMnO_4} + V_{T3})C_{KMnO_4} - 2V_{H_2C_2O_4}C_{H_2C_2O_4}]/V_{aliquot}$$

All the titration methods were tested on model solutions with known concentrations of zinc/aluminum cations or nitrite anions in the range of concentrations 0.1 to 5 mM. The obtained results demonstrated the feasibility of titration technique as analytical method to determine concentrations of the tested ions with an error not exceeding 5 %.

---

<sup>2</sup> The standardized permanganate solution was prepared by boiling a  $KMnO_4$  solution for 1 h followed by aging for 3 days in the dark in a closed glass vessel. The concentration of  $KMnO_4$  was determined by reverse titration with 0.02 M solution of oxalic acid.

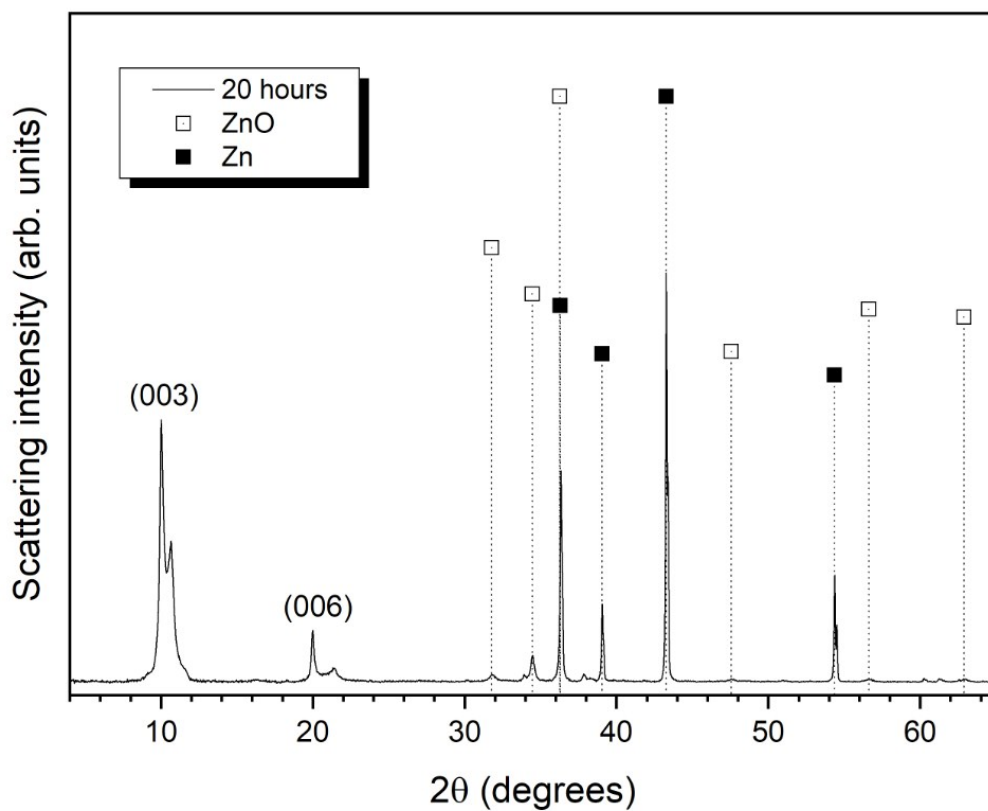


**Fig. S1** XRD pattern of the sample subjected to 20 hours of the treatment. White and black squares designate zinc oxide and metallic zinc phases respectively.

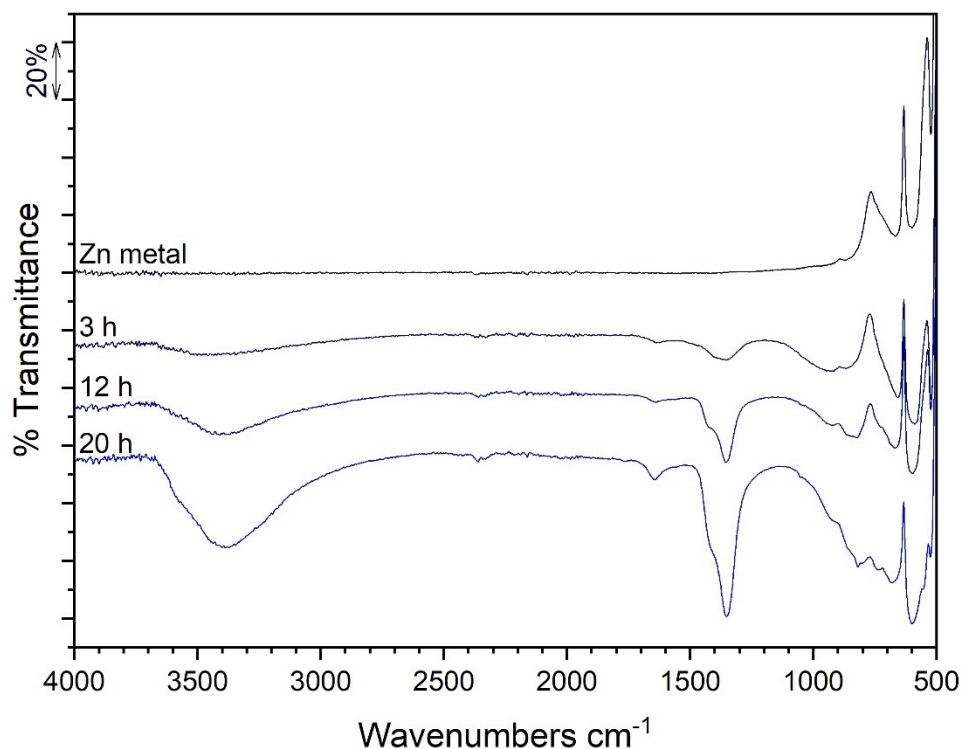


**Fig. S2** FTIR-ATR spectra, taken from a substrate after 3, 12 and 20 hours of treatment as the most representative. The FTIR spectra of ZnAl LDH after 12 and 20 hours of synthesis reveal a strong peak at  $1352\text{ cm}^{-1}$  attributed to the antisymmetric stretching mode of nitrate anion present in LDH. According to the literature<sup>1-3</sup> the strongest vibrational bands of intercalated anions are located in high proximity ( $1365\text{-}1366\text{ cm}^{-1}$  for  $\text{CO}_3^{2-}$ ,  $1370\text{ cm}^{-1}$  for  $\text{OH}^-$ , and  $1351\text{-}1385\text{ cm}^{-1}$  for  $\text{NO}_3^-$ ). A huge signal from different nitrate phases would mask any contribution from a minor phase of carbonate or hydroxide. Other nitrate vibration is visible at  $1052\text{ cm}^{-1}$ , which only becomes IR-active due to the influence of the interlayer confinement<sup>1</sup>. Water vibrations are present as a peak located at  $1644\text{ cm}^{-1}$  (bending mode) and in the region  $3700\text{-}2800\text{ cm}^{-1}$  (O-H stretching mode). To help distinguishing the reflection contribution the spectrum of metallic zinc is presented. Subtraction had not been performed as the reflection impact weakens with time due to the increasing thickness of the coating.

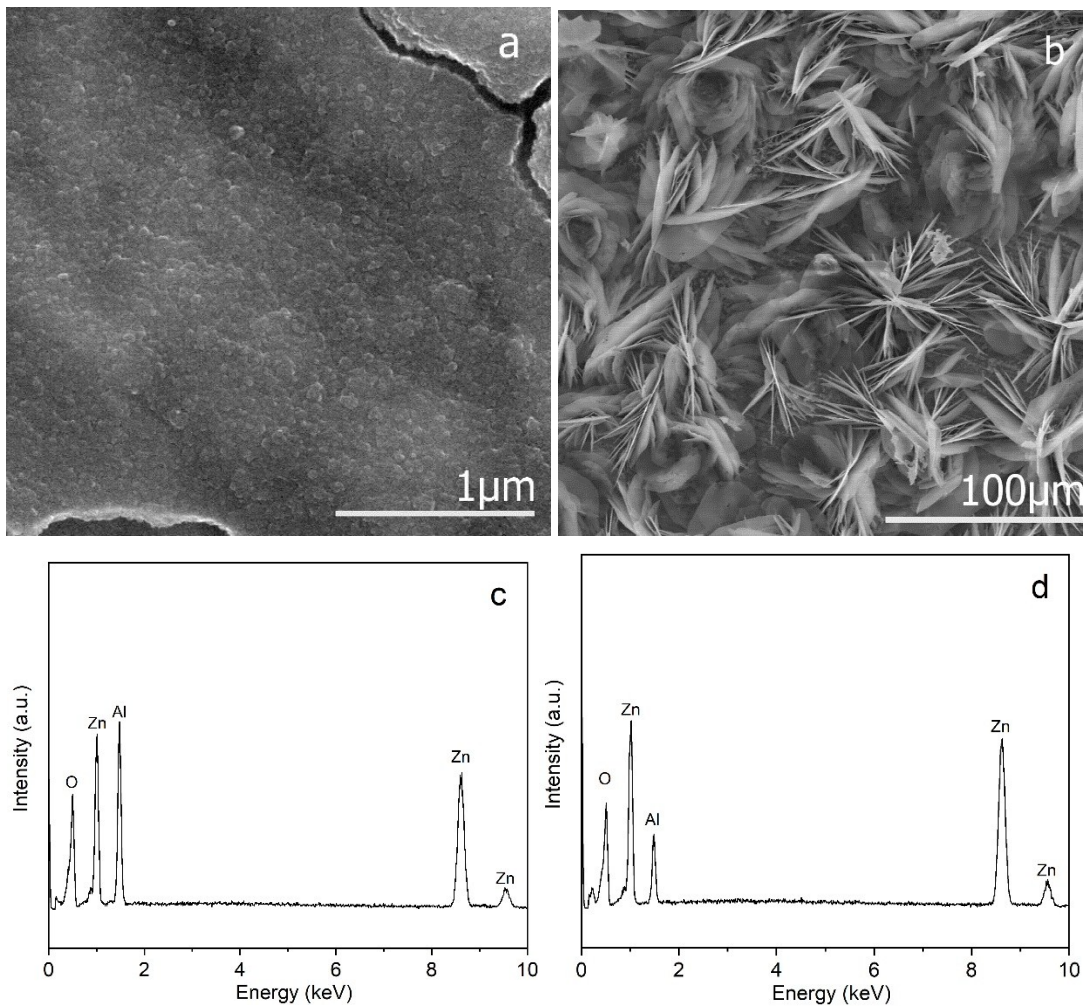


**Fig. S3** a) - SEM micrograph of a surface film deposited on the zinc substrate at 1 hour composed preferably of aluminum hydroxide and b) 20 hours of the treatment; EDS spectra acquired accordingly from the surface after c) 1 hour and d) 20 hours of treatment.

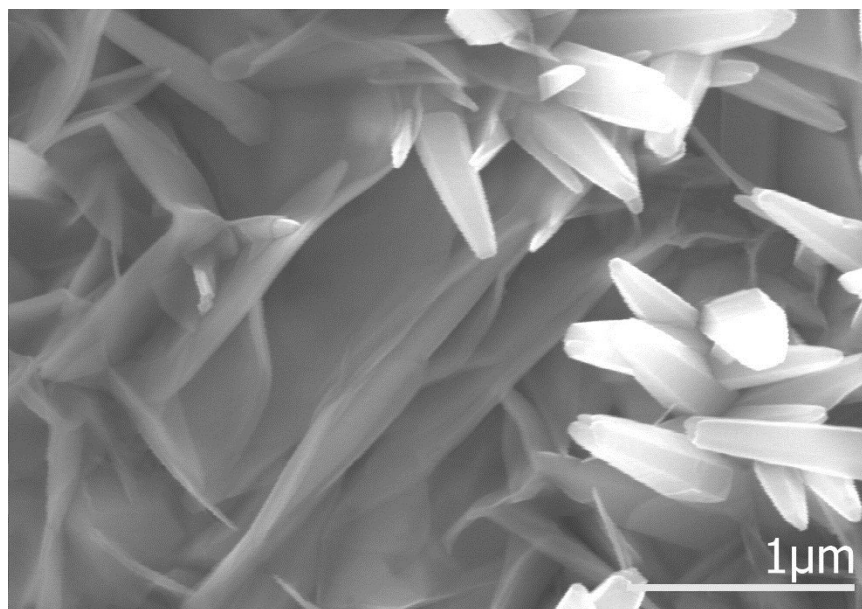


**Fig. S4** SEM micrograph of a zone close to the metal surface. The network of LDH flakes ( $d_1$  phase) is intertwined with hexagonal zinc oxide rod-shaped crystals.



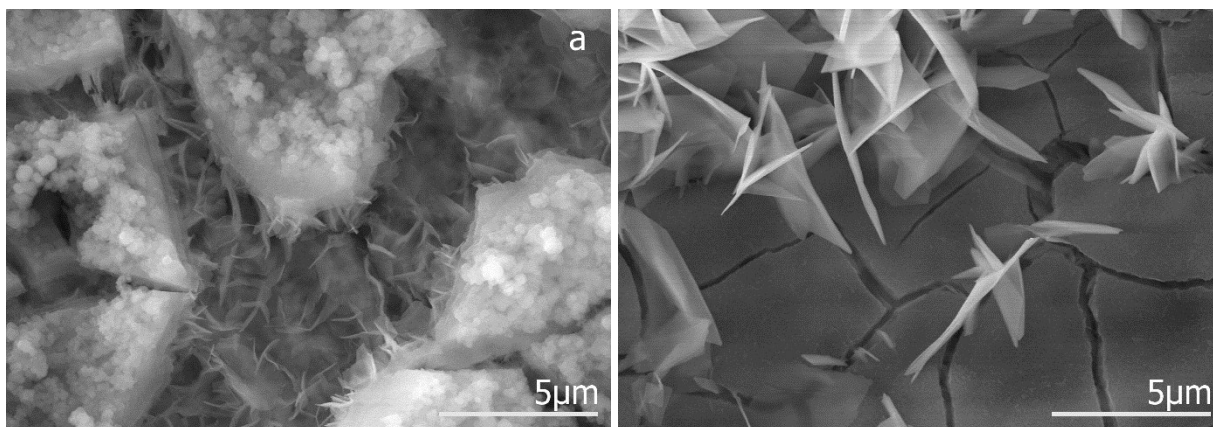


**Fig. S5** a) – SEM image of the zinc surface displaying small LDH crystals (presumably assigned to  $d_1$  phase) in the crack of the hydroxide crust, b) – SEM image revealing the growth of LDH crystals in the crack.

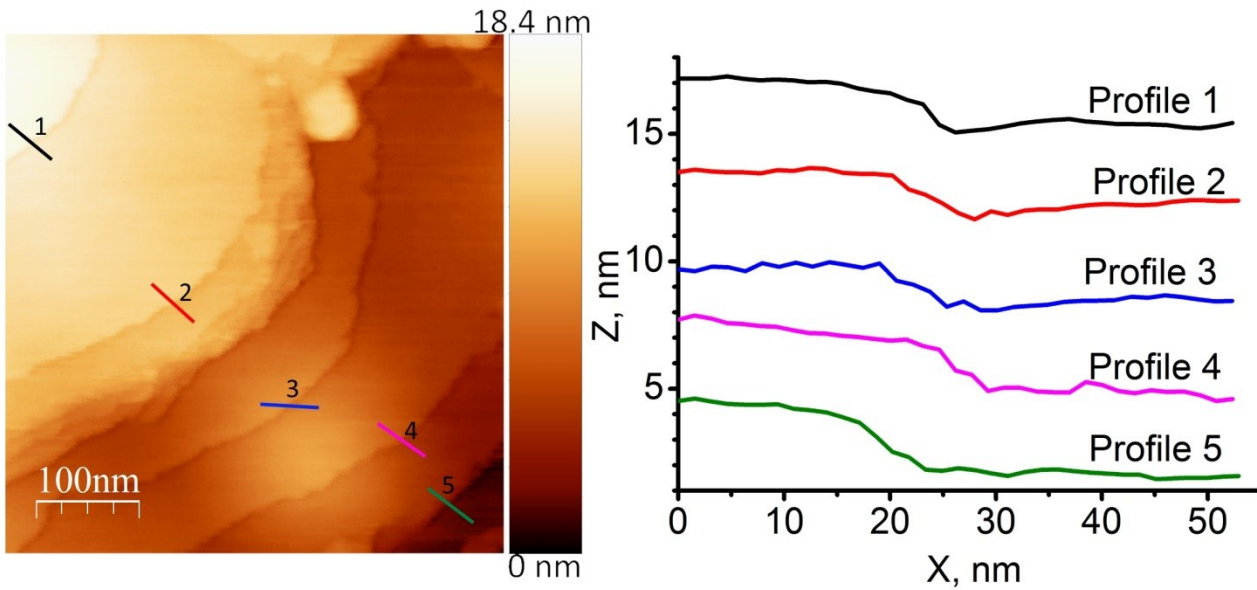


**Fig. S6** a) – AFM topography image taken from the edge of a LDH crystal, b) – topography profiles associated to the image (a) demonstrate well defined steps between different layers of LDH.

Figure S6 depicts potential-pH diagrams for the aluminum-water and zinc-water systems at a temperature of 90°C representing a 3-rd stage of LDH growth described in Figure 3 of this work. The concentrations of zinc and aluminum were 1 mM and 0.05 mM respectively and ionic strength of solution was about 0.1 M. The activities of species estimated according to the Davies Equation. There is a large variety of different thermodynamic data on speciation of condensed and aqueous Zn and Al species, and reaction constants involving such species in literature<sup>4-8</sup>. Therefore, the equilibrium of species at a certain point of pH will depend on which data has been used. However, in order to propose a mechanism of LDH growth we present plausible thermodynamic stability areas of zinc and aluminum species plotted using the Eh-pH module included in HSC Chemistry, mainly using thermodynamic data for Al and Zn species in ref.<sup>7,8</sup>.

Vertical dash lines marked on the diagrams represent experimentally measured pH at 0 h and after 20 h of the synthesis being about 3.3 and 5.9 respectively (90 °C) (Figure S6). The continuous lines on the diagrams represent the Eh-pH-conditions where the content of the adjacent species is the same in the equilibrium state. However, these species always exist on both sides of these lines. Among many possible oxide/hydroxide phases we have chosen ZnO and Al(OH)<sub>3</sub> ones. The rationale for this is that XRD analysis has displayed only ZnO crystalline phase (Figure 1 main text) and none of boehmite or gibbsite crystalline phases attributed to aluminum oxide hydroxides. At the beginning of the synthesis the measured pH of the solution is about 3.2 and both Al and Zn species are preferably in a soluble state (Figure S6 (0h)). While at the end of the synthesis (20 h) the measured pH is in the region where soluble species of Al (Al(OH)<sub>4</sub><sup>-</sup>) and Zn (Zn<sup>2+</sup> and ZnOH<sup>+</sup>) are present (Figure S6 (20h)). At pH close to 6 (90 °C) LDH grows preferably as was determined by XRD studies (Figure 1 main text). Although the measured bulk pH is in the stability area of aluminum hydroxide, the surface pH may substantially increase due to the cathodic processes of oxygen/nitrate/nitrite reduction processes. This plays the key role for shifting the equilibrium towards the soluble species of aluminum needed for LDH growth. On the contrary, at pH < 6 aluminate species precipitate as oxides/hydroxides thus impeding the LDH growth process. While at pH > 6 ZnO preferably precipitates thereby drastically decreasing the concentration of soluble zinc species (Figure S6b) as supported by calculations of Richardson and Lange<sup>7</sup>. Therefore, the favorable conditions for LDH growth are achieved in a slim region of pH where both soluble species of Al and Zn are available.

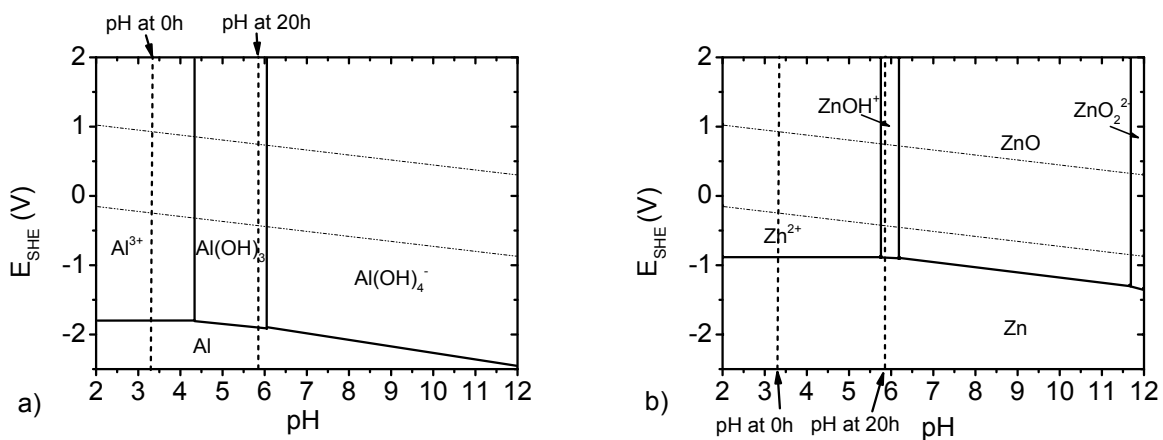


**Fig. S7** Pourbaix diagrams of Al- H<sub>2</sub>O (a) and Zn- H<sub>2</sub>O (b) systems at 90 °C. Dashed vertical lines represent experimentally measured pH (at 90 °C) at the beginning 0 h and after 20 h of the synthesis. The chemical stability area of water is enclosed between the diagonal dotted lines shown in the Eh-pH diagrams.

## References

1. Wang, S.-L. & Wang, P.-C. In situ XRD and ATR-FTIR study on the molecular orientation of interlayer nitrate in Mg/Al-layered double hydroxides in water. *Colloids Surfaces A Physicochem. Eng. Asp.* **292**, 131–138 (2007).
2. Klopogge, J. T., Wharton, D., Hickey, L. & Frost, R. L. Infrared and Raman study of interlayer anions CO<sub>3</sub><sup>2-</sup>, NO<sub>3</sub><sup>-</sup>, SO<sub>4</sub><sup>2-</sup> and ClO<sub>4</sub><sup>-</sup> in Mg/Al-hydrotalcite. *Am. Mineral.* **87**, 623–629 (2002).
3. Kagunya, W., Baddour-Hadjean, R., Kooli, F. & Jones, W. Vibrational modes in layered double hydroxides and their calcined derivatives. *Chem. Phys.* **236**, 225–234 (1998).
4. Shock, E. L., Sassani, D. C., Willis, M. & Sverjensky, D. A. Inorganic species in geologic fluids: Correlations among standard molal thermodynamic properties of aqueous ions and hydroxide complexes. *Geochim. Cosmochim. Acta* **61**, 907–950 (1997).
5. Dirkse, T. P. Zinc Oxide and Hydroxide. in *Copper, Silver, Gold & Zinc, Cadmium, Mercury Oxides & Hydroxides* 156–269 (Elsevier, 1986).
6. Bénézech, P., Palmer, D. A., Wesolowski, D. J. & Xiao, C. New Measurements of the Solubility of Zinc Oxide from 150 to 350°C. *J. Solution Chem.* **31**, 947–973 (2002).
7. Richardson, J. J. & Lange, F. F. Controlling Low Temperature Aqueous Synthesis of ZnO. 1. Thermodynamic Analysis. *Cryst. Growth Des.* **9**, 2570–2575 (2009).
8. Tagirov, B. & Schott, J. Aluminum speciation in crustal fluids revisited. *Geochim. Cosmochim. Acta* **65**, 3965–3992 (2001).